Spectroscopic and electrochemical studies of transition-metal tetrasulfonated phthalocyanines. 3. Raman scattering from electrochemically adsorbed tetrasulfonated phthalocyanines o...

ARTICLE *in* JOURNAL OF THE AMERICAN CHEMICAL SOCIETY · OCTOBER 1985

Impact Factor: 12.11 · DOI: 10.1021/ja00306a007

3 AUTHORS, INCLUDING:

Strahinja Zecevic
Safcell Inc.
49 PUBLICATIONS **1,094** CITATIONS

SEE PROFILE

Spectroscopic and Electrochemical Studies of Transition-Metal Tetrasulfonated Phthalocyanines. 3. Raman Scattering from Electrochemically Adsorbed Tetrasulfonated Phthalocyanines on Silver Electrodes

B. Simic-Glavaski,* S. Zecevic,† and E. Yeager

Contribution from the Case Center for Electrochemical Sciences and the Department of Chemistry, Case Western Reserve University, Cleveland, Ohio 44106. *Received July 20, 1984*

Abstract: Metal-free, cobalt, and iron tetrasulfonated phthalocyanines (H_2-, Co-, and Fe-TsPc) adsorbed on a silver-electrode aqueous interface were studied in situ by resonant and surface-enhanced Raman spectroscopy and cyclic voltammetry. Electrode potential and electrolyte pH were used as experimental variables in oxygen-free media. The silver interface quenches the fluorescence of H_2-TsPc and provides well-resolved Raman spectra for a comparative analysis. Tentative Raman band assignments are provided. A similarity between Raman spectra obtained from solution-phase and adsorbed phthalocyanines suggests a physisorbed mechanism. Anomalously depolarized Raman spectra from the adsorbed phthalocyanines suggest an edge-on model for the macrocycle adsorption orientation. Some Raman bands show a frequency shift as a function of the electrode potential. These shifts correlate with the cyclic voltammogram oxidation peaks. The intensity change of the Raman bands during oxidation-reduction cycles is reversible and accompanied by a hysteresis which is a function of the pH. The intensity changes of the Raman bands during oxidation-reduction cycles are discussed in terms of oxidation-reduction sites on the macrocycle molecule.

Prior preliminary publications from our laboratory on metal-free and transition-metal tetrasulfonated phthalocyanines (H_2-, M-TsPc) have reported the vibrational properties of these molecular species in aqueous solution[1,2] and adsorbed at electrochemical interfaces,[2-5] using resonant Raman and surface-enhanced Raman spectroscopy (SERS). This work involves the more complete studies of the vibrational and the electrochemical properties of these adsorbed macrocycles studied with SERS in combination with cyclic voltammetry on a polycrystalline silver electrode. A fundamental explanatory mechanism for SERS is still wanted but as yet unprovided.[6-8] More recent review papers[9-11] on SERS emphasize that both electromagnetic resonance and electronic resonance mechanisms may be essentially important in promoting SERS. However, SER spectra yield valuable results, and the high signal enhancement factor of about 10^5-10^6 on silver makes SERS a powerful analytical tool for in situ studies of mono- and submonolayer fractions of adsorbed species on this surface. Additional enhancement can be obtained by use of the resonant Raman effect intrinsic to the adsorbed species with SERS, as has already been demonstrated in previous works.[6,12] Although the critical evaluation of the SERS mechanism is not the primary task of this report, recent experimental evidence provides some conceptually new outlooks.

Several research groups have examined the vibrational properties of various phthalocyanines in their solution and crystalline phases[13] and when adsorbed on electrode interfaces.[2,3,14,15] The present work discusses the vibrational properties of adsorbed phthalocyanines on a silver electrode through comparison of a series of phthalocyanine molecules under various electrochemical conditions.

In the present work, the behavior of metal-free, cobalt, and iron tetrasulfonated phthalocyanines as a function of electrode potential was studied on a silver electrode in aqueous solutions of different pH purged with He gas. Both the resonant and nonresonant Raman conditions were involved by using the 632.8-nm He-Ne and 514.5-nm argon ion laser lines, respectively. Raman spectra of the adsorbed Co- and Fe-TsPc molecules on the electrochemical interface are correlated with the Raman spectra obtained from the solid and solution phases of these macrocycle species. Also, Raman spectra with well-defined principal polarization were recorded and yield information on the molecular orientation of the adsorbed macrocycle molecules on the electrode interface. In addition to recording the spectra of the adsorbed species as a function of the electrode constant potential, the intensities of discrete Raman lines were measured during the sweeping of the electrode potential by cyclic voltammetry.

Vibrational Raman data for H_2-TsPc are important for a comparison with similar data obtained for the metallophthalocyanines. Unfortunately, these molecular species in solution and crystalline phases emit strong fluorescence which obscures the Raman signal. However, when H_2-TsPc is adsorbed on silver, the fluorescence is greatly suppressed and it is possible to obtain well-defined Raman vibrational bands.

The influence of sulfonic groups on phthalocyanine molecules has also been examined by comparing the spectra for TsPc with the spectra of the nonsulfonated phthalocyanine adsorbed at monolayer levels in aqueous solutions of various pH.

Experimental Section

Water-soluble metal-free and metallotetrasulfonated phthalocyanines were obtained and purified by using procedures reported by Linstead and

† Permanent address: Faculty of Technology and Metallurgy, University of Belgrade, Belgrade, Yugoslavia.

(1) Simic-Glavaski, B.; Zecevic, S.; Yeager, E. *J. Raman Spectrosc.* **1983**, *14*, 338-341.
(2) Simic-Glavaski, B.; Zecevic, S.; Yeager, E. *J. Electroanal. Chem.* **1983**, *150*, 469-479.
(3) Kotz, R.; Yeager, E. *J. Electroanal. Chem.* **1980**, *113*, 113-125.
(4) Nikolic, B. Z.; Adzic, R. R.; Yeager, E. *J. Electroanal. Chem.* **1979**, *103*, 281-287.
(5) Simic-Glavaski, B.; Zecevic, S.; and Yeager, E.; J. Phys. Chem. 1983, *87*, 4555-4557.
(6) Van Duyne, R. P. In "Chemical and Biochemical Applications of Lasers"; Bradley Moore, Ed., Academic Press: New York, 1979; Vol. 4, pp 101-185.
(7) Furtak, T. E.; Reyes, J. *Surf. Sci.* **1980**, *93*, 351-382.
(8) "Surface Enhanced Raman Scattering"; Chang, R. K., Furtak, T. E., Eds.; Plenum Press: New York, 1981.
(9) Furtak, T. E. In "Advances in Laser Spectroscopy"; Garetz, B. A., Lombardi, J. R.; Eds., Wiley: Chichester, 1983; Vol. 2, pp 175-205.
(10) Chang, K. R.; Laube, L. B. In "CRC critical Reviews in Solid State and Materials Sciences"; CRC Press: Baca Raton, FL, 1984, Vol. 12, pp 1-73.
(11) Otto, A. In "Light Scattering in Solids"; Cardona, M., Guntherodt, G., Eds.; Springer-Verlag: Berlin, 1984; Vol. IV, pp 289-418.
(12) Hagen, G.; Simic-Glavaski, B.; Yeager, E. *J. Electroanal. Chem.* **1978**, *88* (2), 269-275.
(13) Aleksandrov, I. V.; Bobovich, Ya. S.; Maslov, V. G.; Sidorov, A. N. *Opt. Spectrosc.* **1974**, *37*, 265-269.
(14) Melendres, C. A. *J. Phys. Chem.* **1980**, *84*, 1936-1939.
(15) Melendres, C. A.; Rios, C. B.; Feng, X.; McMaster, R. *J. Phys. Chem.* **1983**, *87*, 3526-3531.

0002-7863/85/1507-5625$01.50/0

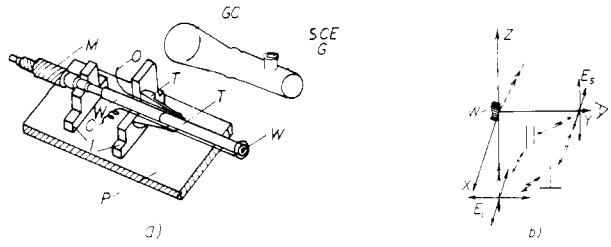

Figure 1. (a) Electrochemical cell for simultaneous Raman scattering measurements. G is the glass cylinder, GC is the connecting glass cone, SCE is the inlet for the saturated calomel electrode, M is the nonrotating micrometer head, W is the working electrode, O is the gas inlet, T is the Teflon body, C is the counterelectrode, I is the insulating supports, and P is the cell platform. (b) Schematic presentation of the electrode surface illumination and the orientations of the incident laser $\vec{E}_i$ and the scattered light $\vec{E}_s$ electric field vectors. The propagation of the laser light is along the Z axis and the observation of the scattered light is along the Y axis. The normal of the electrode surface is in the ZOY plane.

Weiss[16] and Weber and Busch,[17] respectively. Other materials were of ultrapure reagent grade.

The Raman cell–electrode assembly, together with the optical illuminating geometry, is shown in Figure 1. The electrode surface parallel to the quartz window can be precisely positioned, and the volume between the electrode surface and the scattering window can be varied and minimized. The silver disk electrode of 0.63-cm diameter was mounted in a Teflon holder which was, in turn, mounted on the nonrotating micrometer head (see Figure 1). A platinum counterelectrode and gas feed were supported through the main Teflon body which holds the glass cell. A reference-saturated calomel electrode (SCE) was connected to the cell electrolyte through a stopcock salt bridge of 0.05 M Na_2SO_4 at the top opening of the cell. The electrolyte was in contact only with the glass and Teflon parts of the cell plus the working electrode and counterelectrode. The potential of the electrode was controlled with a potentiostat Pine Model RDE 3. This electrochemical-optical cell was then mounted on a micropositioning platform with 3 orthogonal degrees of freedom, which could provide various illuminating geometries.

The surface of the working electrode or the silver electrolyte interface was illuminated with a He–Ne laser (Spectra-Physics Model 125) with an output power of about 40 mW operating at 632.8 nm. The He–Ne laser excitation line falls within the Q band[2] of the visible absorption spectra of the phthalocyanine and hence satisfies the requirements for resonant and preresonant Raman excitation. The argon ion laser (Coherent Radiation 54G) provided nonresonant excitation lines at 514.5 and 488.0 nm with reduced output powers at about 100 mW which were used for nonresonant SERS. The laser plasma lines were eliminated by filtering the laser output through a prism monochromator.

The plane of polarization of the laser radiation was rotated with a wide-band polarization rotator (Spectra-Physics Model 310), and the polarized and depolarized laser light scattered from the interface was collected through a Polaroid analyzer. As a check on the system, the CCl_4 459-cm^{-1} Raman band was used as a reference and found to be proper. The Raman scattered light was analyzed by a double monochromator (Spex 1400), photomultiplier (ITT FW130), and a photon counting system. Some Raman data were also obtained with a Spex Triplemate and an optical multichannel analyzer which employed a diode array detection system (Tracor Northern).

The working polycrystalline silver electrode was polished mechanically with Al_2O_3 of 0.05-μm grain size to provide a mirrorlike surface finish and then washed with distilled water. The electrode surface was then exposed to ultrasonic waves in distilled water to remove any trace of aluminum oxide particles from the surface of the silver. The appropriate electrolyte was added in the assembled optical-electrochemical cell with TsPc at a 10^{-5} M concentration. Then the nonilluminated electrode was subjected to anodization or roughening by keeping it at an anodic potential of +0.45 V for 30 s. The Raman signal was generally the largest after activation of the electrode. The additional cycling of the electrode potential between, e.g., 0.2 V and H_2 evolution potential, with a sweep rate of 100 mV/s, irreversibly decreased the Raman signal which approached a steady level after about 10–20 min. If the electrode was not cycled after the activation, the Raman signal also irreversibly decreased to a steady value after 10–20 min and remained at this level for at least several hours. Such stability and reproducibility of the optical signal within the error margin of 10% was necessary for the recording and

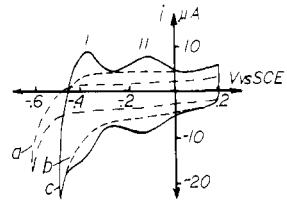

Figure 2. Cyclic voltammograms obtained from (a) pure silver, (b) silver after anodic activation at 0.45 V vs. SCE for 30 s, and (c) adsorbed Fe–TsPc. Supporting electrolyte: 0.05 M H_2SO_4 purged with He. Electrode area: 0.31 cm^2. T = 20 °C. Potential sweep rate: 100mV/s.

comparative analysis of the spectra.

Various workers have found that the silver electrode anodization or roughening is necessary for strong SERS.[6-11] However, strong SERS can also be obtained without anodic activation if the silver surface is potentiostated at −1.5 V vs. SCE for about 1 min. One can observe hydrogen evolution during such cathodic activation, but there are no visible changes on the silver electrode surface.

At this point, it may be appropriate to comment on the effects of the activation procedure and the deposition of TsPc on the polycrystalline silver electrode.

Typical cyclic voltammograms of the blank and activated silver electrode are shown in Figure 2. Figure 2 includes also a cyclic voltammogram obtained from the adsorbed Fe–TsPc. Two redox peaks are associated with the oxidation–reduction of the principal phthalocyanine ring; both peaks are characteristic for both metal-free and metallophthalocyanines. Data obtained from the cyclic voltammograms indicate that the adsorbed TsPc was in the form of a monolayer with an average surface coverage of about 10^{-10} M/cm^2. A detailed analysis of adsorbed TsPc on electrode surfaces by cyclic voltammetry will be reported elsewhere.[18]

In general, a twofold increase in a double layer capacitance has been observed after the anodic activation, indicating an increase of the effective surface area (see Figure 2, curve b). The mirrorlike shine of the electrode surface did not change during such activation. Van Duyne[6] reported that the surface roughness is composed of silver particulates larger than 250 Å.

The cathodic activation showed virtually no change in the double-layer capacitance (see Figure 2, curve a) in contrast to the anodic activation procedure. Also, one had an impression that the shine of the electrode surface area increased. This suggested that the cathodic activation produced less roughened surface of the electrode.

Examinations of the surfaces were performed visually by using a low magnification lens in order to detect physical damage or burning spots on the electrode surface. Such changes were not detected.

A detailed examination of the surface morphology by electron microscopy was not the objective of this work, and therefore it was not carried out.

After cathodic activation (just as with anodic activity), the stabilization of the Raman signal requires several voltage sweeps and about 10–20 min at a given solution for the Raman signal to decrease to a stable value. These facts indicate that the time factor is predominant in the stabilization of the optical signal.

Our recent experimental evidence shows that the Raman signal enhancement can be obtained from the adsorbed TsPc on single-crystal silver electrode interfaces which have not been electrochemically activated or roughened but only exposed to laser light. This photopromoted Raman enhancement is fundamentally important and shows that the roughening of the silver surface is a secondary effect of the processes which promote SERS and that the physical morphology of the surface is not of the primary concern. Critical evaluation of the photopromoted Raman enhancement will be reported elsewhere.[19]

After the Raman signal had stabilized, the electrolyte containing the 10^{-5} M TsPc was always removed and the cell then rinsed and filled with a solution free of TsPc. Thus, the only TsPc molecules were only strongly attached at the electrode surface. The Raman signal was more intense with the solution containing no TsPc since the losses associated with solution absorption were no longer involved.

Results and Discussion

1. Raman Spectra from the Adsorbed Phthalocyanines. The spectra of the preresonant and the resonant Raman light scattered

(16) Linstead, R. P.; Weiss, F. T. *J. Chem. Soc.* **1950**, 2975–2981.
(17) Weber, J. H.; Busch, D. H. *Inorg. Chem.* **1965**, *4*, 469–497.
(18) Zecevic, S.; Simic-Glavaski, B.; Yeager, E.; Lever, A. B. P.; Minor, P. *J. Electroanal. Chem.*, submitted.
(19) Simic-Glavaski, B., unpublished results.

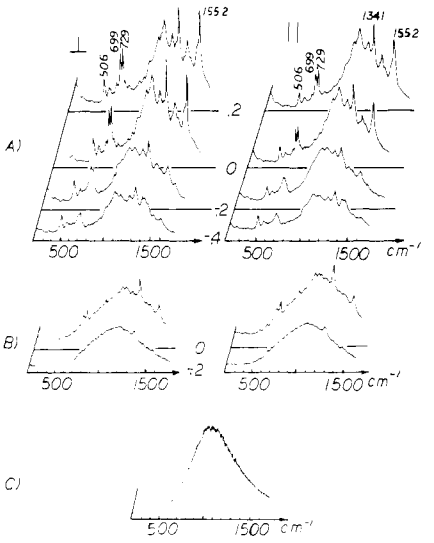

Figure 3. Resonantly surface enhanced Raman spectra obtained from the adsorbed H_2–TsPc on silver electrode for the depolarized ⊥ and the polarized II scattered light at various electrode potentials in (a) acidic, pH ~1, (b) neutral, pH ~7, and (c) alkaline, pH ~13, media. The laser excitation was at 632.8 nm and 20-mW output power. Resolution 2 cm^{-1}; scanning time 10 min/spectrum. The electrolytes were saturated with He gas, and the experiments were conducted at room temperature, T = 20 °C. The intensity was 50 000 counts/s full scale. Potentials of the working electrode vs. SCE in volts are indicated along wavenumber axes. The depolarized and polarized light scattering configurations shown in Figure 1b were used for recording the spectra in Figures 3, 4, 5, and 10.

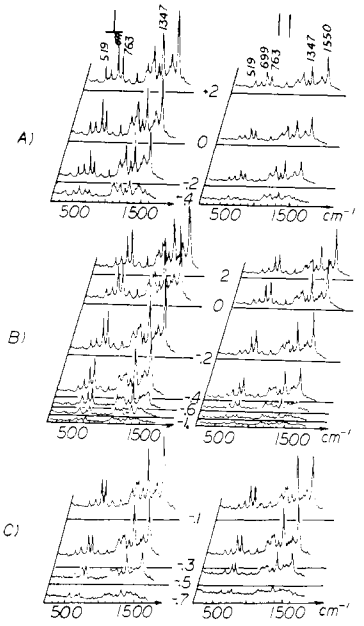

Figure 4. Same as in Figure 3 but for the adsorbed Co–TsPc on the silver electrode.

from the adsorbed molecules of H_2–TsPc, Co–TsPc, and Fe–TsPc on the silver electrode were recorded in both the polarized and depolarized light-scattering configurations at various electrode potentials and in three principal pH media. Raman spectra from the adsorbed macrocycle molecule are shown in Figures 3–5 for acidic (0.05 M H_2SO_4; pH ~1), neutral (0.05 M Na_2SO_4; pH ~7), and alkaline (0.1 M NaOH; pH ~13) environments. It is important to note that the three potential sweeps between +0.2V and H_2 generation potentials were performed only once before each set of the spectra displayed in Figures 3–5. An intermediate additional cycle of the electrode produces spectra of different intensities and hence is unsuitable for a comparative study of the spectral changes as a function of the electrode potential.

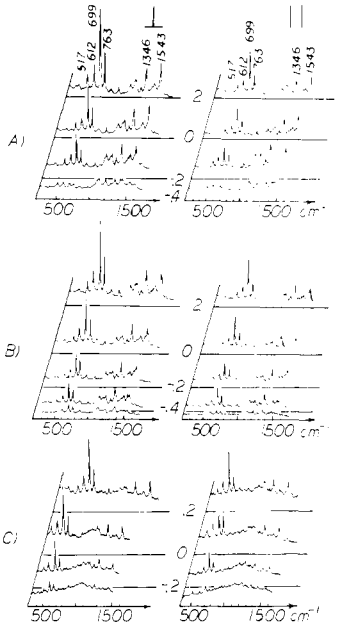

Figure 5. Same as in Figure 3 but for the adsorbed Fe–TsPc on the silver electrode.

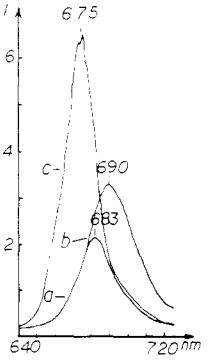

Figure 6. Fluorescence profiles from the aqueous solution phases of 10^{-6} M H_2–TsPc in (a) acidic 0.05 M H_2SO_4 (pH ~1) aqueous electrolyte, (b) neutral 0.05 M Na_2SO_4 (pH ~7) aqueous electrolyte, and (c) alkaline 0.1 M NaOH (pH ~13) aqueous electrolyte. Intensity scale is in 10^4 counts/s; laser excitation is 632.8 nm with 20-mV output power.

The base lines in the displayed spectra correspond to the level of white noise measured at about 4000 cm^{-1} away from the incident laser radiation.

Several interesting features can be immediately recognized. Resonant and preresonant Raman spectra from the adsorbed macrocycle molecules on silver electrodes are similar in appearance to those spectra obtained from the aqueous solution phases,[1] with the exception of H_2–TsPc which emits fluorescence in similar media. A strong preresonant fluorescence from the aqueous solution phase of H_2–TsPc overpowers the Raman scattering signal. The fluorescence is intense even at the concentration of 10^{-6} M of H_2–TsPc in the solution phases, with the corresponding spectra shown in Figure 6. A fluorescence peak occurs at 690.4 nm for pH ~7, which is in good agreement with the previously reported value.[20] The fluorescence emission from H_2–TsPc adsorbed on various interfaces will be discussed in a later report.[21]

The fluorescence from H_2–TsPc adsorbed on the silver in an acid medium is quenched, and the Raman scattering signal appears stronger with fully resolved vibrational bands. The quenching of the fluorescence by silver is far less in other media. This can be explained in terms of a change in the nature of the interaction of the TsPc with the silver surface. Such a change in interaction may occur because of the loss or gain of inner protons.

(20) Allison, J. B.; Becker, R. S. *J. Chem. Phys.* **1960**, *32*, 141–1417.
(21) Simic-Glavaski, B.; Zecevic, S.; and Yeager, E., unpublished results.

Cotton et al.[22] have proposed that the fluorescence quenching for adsorbed tetrasodium *meso*-tetrakis(4-sulfonatophenyl)-porphyrin is due to silver incorporation in the inner macrocycle ring during the anodic activation of the silver electrode. Fluorescence quenching was also observed in the present study when the anodic activation of the silver was carried out with the TsPc only being added subsequently and even when there was no activation of the silver at all.

Resonant and preresonant Raman scattered light from the adsorbed TsPc on the silver electrode was intense and was normally in about the range of about 20 000 counts/s for the most intense Raman peaks while from the solution phases the same signals were in the range of 200–300 counts/s. Assuming that the origin of the scattering is a monolayer of the adsorbed species, then one obtains an effective gain of about 10^7 at the same laser excitation power. This gain is principally as a result of the resonant surface enhancement mechanism. The gain factor is estimated on the basis of a surface concentration of 1.6×10^{-10} mol/cm^2 (evaluated from linear sweep voltammetry) with a reasonable estimate of the surface area of the electrode and volume of the solution from which the Raman radiation was collected in the two sets of measurements.

The spectral data given in Figures 3–5 were obtained from electrodes prepared in the manner described in the Experimental Section. It should also be noted here that, if the Raman spectra are recorded at a given electrode potential, then it appears that the Raman bands and spectra from the adsorbed TsPc are invariant to the prior potentials at which the macrocycle molecules have been preadsorbed. The preadsorption of the TsPc can be safely performed within the potential range between -1.5 and 0.6 V without any distortion of the molecular structure, indicating its high stability vs. the potential of the electrode.

Other important information is frequently missed in the reports on SERS which are related to the silver relative gain factor. The gain is not uniquely defined and is greatly influenced by experimental conditions. However, if the experimental conditions are constant and if the experimentalist follows his own set of standards, then very high reproducibility of data can be achieved. For example, an additional gain of nearly an order in magnitude can be obtained if the electrode is anodized at higher potentials (0.6 V). Such an anodization significantly alters the mirrorlike electrode surface. The surface appears as a white powdered highly roughened structure. The spectral features of the adsorbed TsPc are unaltered, but the gross scattering signal is unstable and rapidly decreases in the intensity. Electrode surfaces so superactivated were not used in the comparative analysis.

The adsorbed phthalocyanines without sulfonic groups were also studied in order to determine the effect of sulfonation on the overall macrocycle behavior. The vibrational modes associated with the sulfonic acid groups are apparently not resonantly enhanced.

RSER spectra obtained from the adsorbed Pc and TsPc are very similar though these show some slight differences in the band positions which are below 1000 cm^{-1}. The frequency shifts in the band positions are most probably caused by a dipyridine axial complex. Such a strong complex is usually formed when the Pc is dissolved in the pyridine solvent, and such solution is then used to deposit Pc on the silver electrode.

A detailed analysis of the recorded Raman bands originating from the adsorbed macrocycle molecules in acidic (pH $\sim$1), neutral (pH $\sim$7), and alkaline (pH $\sim$13) media showed no detectable change in their position as a function of pH; however, it is possible that frequency shifts could have been within the resolution of the measurements ($\pm$2 cm^{-1}). On the other hand, the intensities of the Raman bands show considerable dependence on pH which is to be expected since the UV–visible absorption spectra are quite pH-dependent.

The positions of the Raman bands observed from the TsPc adsorbed on the silver electrode and in aqueous solution phases, from Pc adsorbed on a silver interface and dissolved in tetrahydrofuran (THF),[13] and from crystalline Pc[13] as well as the corresponding infrared spectral data[23] are summarized in Table I. A tentative band assignment of the vibrational modes was performed through a comparative analysis and the use of previous band assignments for the pyrrole[24] and benzene rings.

Resonantly surface-enhanced Raman spectra from the adsorbed TsPc on the silver electrode are very similar in shape and band position to those spectra reported from aqueous solutions,[1] suggesting that physisorption is more likely than chemisorption.

The correlations between data from Pc dissolved in THF, solid Pc, and our data are in good agreement. It is also important to note that the Raman bands obtained from the TsPc adsorbed on silver overlap very well with the corresponding Raman bands obtained from ferrocytochrome *c*,[25,26] hemoglobin[26], and porphyrin[27] molecules. In the spectra from these macrocycle molecules, the most predominant Raman bands originate from the pyrrole vibrations.

The frequency range between the Rayleigh line and 200 cm^{-1} was also examined in this study. A number of very weak bands were observed which could not be positively assigned. As pointed out by Spiro,[25] metal–nitrogen stretches and their corresponding Raman bands would be of considerable interest and significance; however, their identification appears to be elusive. Abe's[28] calculation of normal-mode frequencies for nickel octaethylporphyrin predicts two active metal–nitrogen modes ν_{18} at 187 and ν_{52} at 264 cm^{-1}. It is conceivable that the observed Raman bands at 255 and 241 cm^{-1} may represent Co–N and Fe–N vibrations, respectively, for the adsorbed Co–TsPc and Fe–TsPc on the Ag electrode. This assumption may be correct since the Raman data obtained from the adsorbed Fe–Pc most probably is in the form of a dipyridine axial $(py)_2$Fe–Pc complex which shifts the band at 241 cm^{-1} to a new value of 268 cm^{-1}.

The group of Raman bands between 400 and 700 cm^{-1} represent a pyrrole out-of-plane folding deformation and are more pronounced in the spectra obtained from Fe—TsPc, while the bands at about 1350 and 1550 cm^{-1} represent C—N and C=C breathing and stretch vibrations and are more characteristic for the spectra obtained from H_2—TsPc and Co—TsPc. This kind of spectral behavior is not unexpected if one considers the possible motion of the central metal ion in the inner ring. In studies of octaethylporphyrins[29] and heme molecules,[30] out-of-plane vibration of iron can form a domed structure and therefore influence the pyrrole ring deformational modes. Spaulding et al.[29] estimate that the amplitude of iron displacement may vary between 0.21 and 0.475 Å and that the iron ion can assume several different spin values. On the other hand, the vibrations of protons or cobalt are in the plane of the inner ring; these can affect pyrrole stretching modes at about 1350 and 1550 cm^{-1}.

The breathing mode at about 1350 cm^{-1} is frequently called an oxidation marker band. Spiro and Strekas[31] propose a possible electron exchange between the iron ion and π orbitals which in turn may cause a frequency shift of that Raman band. However, this may be considered a contraversial[29,32] issue.

2. Depolarization Effects. One of the most interesting phenomena associated with the Raman scattering from interfaces involves the question of the unusual depolarization effect. Nu-

(22) Cotton, T. M.; Schultz, S. G.; Van Duyne, R. P. *J. Am. Chem. Soc.* **1982**, *104*, 6528–6532.

(23) Sidorov, A. N.; Kotlyar, I. P. *Opt. Spectrosc.* **1961**, *11*, 92–96.
(24) Lord, R. C.; Miller, F. A. *J. Chem. Phys.* **1942**, *10*, 328–341.
(25) Spiro, T. G. In "Iron Porphyrins"; Lever, A. B. P., Gray, H. B., Eds.; Addison-Wesley Publishing Co.: London 1983; Part II, pp 89–159. Spiro, T. G.; Strekas, T. *Proc. Natl. Acad. Sci. U.S.A.* **1972**, *69* (9), 2622–2626.
(26) Bruner, H. *Biochem. Biophys. Res. Commun.* **1973**, *51* (4), 888–894.
(27) Verma, A. L.; Bernstein, H. J. *Biochem. Biophys. Res. Commun.* **1974**, *57* (1), 255–262.
(28) Abe, M.; Kitagawa, T.; Kyogoku, Y. *J. Chem. Phys.* **1978**, *69*, 4516–4524.
(29) Spaulding, L. D.; Chang, C. C.; Yu, N. T.; Felton, R. *J. Am. Chem. Soc.* **1975**, *97* (9), 2517–2225.
(30) Stein, P.; Burke, J. M.; Spiro, T. G. *J. Am. Chem. Soc.* **1975**, *97* (8), 2304–2305.
(31) Spiro, T. G.; Strekas, T. C. *J. Am. Chem. Soc.* **1974**, *96*, 338–345.
(32) Kitagawa, T.; Ogoshi, H.; Watanabe, E.; Yoshida, Z. *J. Phys. Chem.* **1975**, *79*, 2629–2635.

Table I[c]

	Co–TsPc		Co–Pr				Fe–TsPc		Fe–Pc				H_2–TsPc		H_2–Pc				pyrrole		assign-
	on Ag	in H_2O	in THF[a]	on Ag	solid[a]	IR[b]	on Ag	in H_2O	in THF[a]	on Ag	solid[a]	IR[b]	on Ag	in H_2O	THF[a]	Ag	solid[a]	IR[b]	*d*	*c*	ment
1	255						241			268											
2	344						332	327													
3	387			387			387	394					366	F	N	N					
3a						434						435						434			
4	519	518		498		520	517	523		493		518	506	L	O	O		492			χ_R
5	570			577		575	570					575	570					557			
6	610	612	593	598	593		612	616	587	598	596		624	U				620	586	585	χ_{HH}*
7	699	699	686	690	687	647	699	699	679	690	644	644	699				683		664	646	χ_R*
8	729	722				726	728	726	738			726	729	O			725	714	734	711	σ_R
																		736			
9			753	758	752	756				754	755	756	754					753			
10	763	765				772	763	767		785	780	771		R	D	D		766		768	*
11						780						780	799					778			
11a						804						804		E			800				
12	866	866	837	839	831	868	866	870	830	846	833	868			A	A		870	866	866	χ_{CH}
12a						877						877	891					880			
														S							
12b						915						910	911					914			
13	948			920		948	944			926		948		C	T	T		946			
14	981	983	962	968	960	956	977	983		964	951		968					958			
15									1007					E				1007			
16	1040			1014		1078	1040			1016		1072	1038		A	A	1030		1078	1072	σ_{CH}
16a						1092						1089		N				1094			
17	1114	1118	1114	1116	1108	1102	1112		1102	1118	1110	1121	1123				1085				
18	1136	1133	1141	1144	1140	1121	1136	1144	1156	1142	1147	1165		C			1142	1119	1138	1144	ν_R
18a						1165												1160			
19	1194	1204		1206		1174	1196	1208		1208	1200	1173	1185	E				1163			
20	1225	1229	1215	1230	1215		1223	1223		1230									1237	1237	δ_{CH}
21	1284	1289	1281	1284	1308	1291	1285	1285	1286	1283		1290	1283					1277			
21a																		1304			
21b										1312								1321			
22	1347	1352	1348	1347	1348	1334	1346	1352		1341	1343	1333	1341					1336	1392	1379	ν_RN—C
23	1408	1412		1406						1366										1418	
24	1437		1440	1436		1428	1433			1437	1422	1429	1429					1439			
25	1467	1476		1466	1465	1471	1462	1476	1445	1456	1450	1468						1461	1474	1467	ν_R
26	1488					1487	1489		1484	1476		1484						1478			
27				1521		1526	1515			1511	1520	1516	1521					1503			
28	1550	1551	1535	1546	1540		1543	1551		1535			1552				1544		1530	1532	C=C*
29				1592		1597	1595			1592		1592						1600			
30	1611					1612	1604					1609	1620					1617			

[a] Aleksandrov, I. V.; Bobovich, Ya. S.; Maslov, V. G.; Sidorov, A. N. *Opt. Spectrosc.* **1974**, *37*, 265–269. [b] Sidorov, A. N.; Kotlyar, I. P. *Opt. Spectrosc.* **1961**, *11*, 92–96. [c] Lord, R. C.; Miller, F. A. *J. Chem. Phys.* **1942**, *10*, 328–341. [d] Simic-Glavaski, B.; Zecevic, S.; Yeager, E. B. *J. Raman Spectrosc.* **1983**, *14*, 338–341. [e] χ out-of-plane bending mode, δ in-plane bending mode, and ν stretching mode. An asterisk indicates the principal strongest bands.

merous reports on SERS[6-11] have indicated that the majority of SER spectra are depolarized. This scattering effect of interfaces is not a novel one[33] and is often a subject of different hypothesis.[34-36]

Depending on the conventions[37] of the scattering geometry used in experiments, one observes the four scattering spectral components as summarized below:

$$I_{SS} = I_{VV} = I_{XX} = I_{\parallel}$$

$$I_{SP} = I_{VH} = I_{XZ} = I_{\perp}$$

$$I_{PS} = I_{HV} = I_{YX} = I_{\perp}$$

$$I_{PP} = I_{HH} = I_{YZ} = I_{\perp}$$

The components are defined according to the polarization state of the incident and scattered light in a laboratory system as displayed in Figure 1b where the first and second indexes refer to the direction of the electric vector in the incident and the scattered light, respectively.

This frame of reference in space can provide information on orientation in space of the molecular-induced dipole moment.

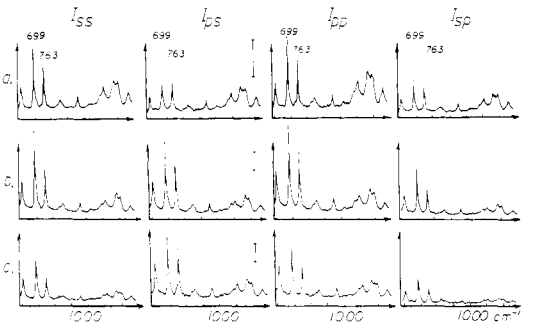

Figure 7. Four principal Raman components recorded from adsorbed Fe–TsPc on polycrystalline silver. The principal Raman bands are indicated in inverse centimeters. (a) Multilayered (about 100 layers) structure of adsorbed Fe–TsPc on silver–air interface. (b) Same structure but the interface is in 0.05 M H_2SO_4 aqueous electrolyte. The spectra were recorded 30 min after the replacement of the air by the aqueous electrolyte interface. Open-circuit potential. (c) Spectral components obtained from the same Ag|Fe–TsPc|electrolyte interfaces as in (b) but after 60 min. The spectral components were recorded with the Spex Triplemate monochromator of 10-cm^{-1} resolution and diode array multichannel optical analyzer Tracor Northern Model 1710. Laser excitation: 20 mW at 632.8 nm. Vertical bar indicates a relative unit of the light scattered intensity.

In standard Raman scattering from bulk media, the component with parallel electric vectors is the most intense and is often

(33) Raman, C. V.; Ramadas, L. A. *Proc. R. Soc. London* **1925**, *108*, 561–571.
(34) Lao, U.; Schatz, G. C. *J. Chem. Phys.* **1982**, *76* (6), 2888–2899.
(35) Moskovits, M. *J. Chem. Phys.* **1982**, *77* (9), 4408–4416.
(36) Gersten, J.; Nitzan, A. *J. Chem. Phys.* **1980**, *73* (7), 3023–3037.
(37) Berne, J.; Pecora, R. "Dynamic Light Scattering with Application to Chemistry, Biology and Physics"; Wiley-Interscience: New York, 1976.

referred to as the polarized component; those components with perpendicular electric vectors are less intense and called the depolarized components. It should also be mentioned here that the Krishnan[38] principle of reversibility $I_{SP} = I_{PS}$, though usually valid for Raman scattering from bulk media, is not necessarily valid for Raman scattering from interfaces.

The four Raman spectral components and their intensities shown in Figure 7 illustrate the experimental conditions and the orientation of the adsorbed TsPc on the solid substrate.

The Raman components in Figure 7a were obtained from about 100 monolayers of the adsorbed Fe–TsPc on the silver surface interfaced with air. The multilayered structure Ag|(Fe–TsPc)$_{100}$|air is formed by depositing a droplet of about 3 μL of 10^{-3} M Fe–TsPc on silver surface of 0.3-cm^{-2} geometric area. This amount of the deposited Fe–TsPc, corresponds after the solvent evaporation to 10^{-8} M Fe–TsPc/cm^2. The most intense component is $I_{pp} = I_{HH}$, and it is approximately equal to the I_{SS} component with the ratio of $I_{PS}/I_{SS} < 1$ and $I_{PS} \approx I_{SP}$. The subsequent sets of Raman components shown in Figure 7b were obtained from the multilayered structure on interface of Ag|(Fe–TsPc)$_{100-n}$|0.05 M $H_2SO_4 + H_2O$. The spectra were recorded about 30 min after the replacement of the air by the electrolytic interface; n represents the time-dependent number of dissolved layers from the interface.

As time elapsed, the intensities of the spectral components changed to the levels shown in Figure 7c, indicating a significant alteration in the spectral components which are related to a number of the adsorbed layers.

It is important to note that the intensity scale in Figure 7a is twice as sensitive as in Figure 7b and c.

An increase, almost twofold, in the level of the scattering signal in Figure 7b and c can be explained in terms of the distance-dependent surface enhancement factor which was also reported recently by Goncher et al.[39] The surface enhancement factor is inversely correlated with the closeness of the adsorbed molecules to the silver surface. Also, a self-absorption of the outer layers significantly reduces the scattering intensity of the first layers. The intensity changes in the spectra displayed in reduces 7 are to be expected.

The intensity levels of the Raman components shown in Figure 7c are very similar to the intensity of the components obtained from a deposited 3 μL of 10^{-5} M Fe–TsPc on a silver surface. This amount of $\sim 10^{-10}$ M Fe–TsPc/cm^2 is in good agreement with the value of 1.6 10^{-10} M Fe–TsPc/cm^2 calculated from the area of the redox couples of the adsorbed Fe–TsPc on the silver electrode measured by cyclic voltammetry. Assuming that redox couples obey the Nernst equation, then one obtains the value of about 0.8 which indicates that one electron is involved in each of the surface redox processes and that the electrode coverage corresponds to a monolayer.

The similarity between the intensities and their ratios of the Raman components in Figure 7c and Figure 4 and those of the components obtained from 10^{-10} M Fe–TsPc/cm^2 on a silver electrode convincingly suggests that the spectra already shown in Figures 3, 4, and 5 are obtained from the monolayer of the adsorbed TsPc on the silver electrode.

The intensity levels of the Raman components shown in Figure 7a can be obtained also from electrochemically deposited TsPc on the silver electrode, if the electrode activation is performed at 0.6 V vs. SCE for about 30–40 s with TsPc present in the electrolyte. The Raman scattering signal irreversibly changes with time or with a more negative electrode polarization and reaches the levels shown in Figure 7c. This trend in the change of the Raman intensity components actually describes the unstable multilayered structure and its alteration when the silver electrode interface is superactivated.

Similar effects were observed for other macrocycle molecules deposited on the silver surface under the same experimental conditions and by using nonresonant laser lines.

Theoretical models used to explain the unusual depolarization effect of interfaces do not find full support in the example of the adsorbed phthalocyanine molecules. The model of Lao and Schatz[34] involves coupling of dipoles with randomly distributed spheroids on the silver electrode. According to Moskovits,[35] selection rules for the adsorbed molecules would promote only the I_{PP} component, though, other components would be non-zero for nonideal surfaces. The model of the orientated dipole of Gersten and Nitzan[36] appears to be the most appropriate one. These authors calculated that the silver enhancement factor for the normal orientation of the dipole on a surface may be several orders greater than the corresponding enhancement factor for the parallel orientation of the dipole with respect to the electrode surface.

The model of Spiro and Strekas[31] involving a change of polarizability tensors for the adsorbed phthalocyanines molecular species is very unlikely. This model would require a substantial change of molecular symmetry during the process of the adsorption. The experimental evidence obtained in this laboratory rules out that possibility. The symmetry of TsPc appears to be unaltered during the adsorption processes and remains the same in solution phases and for the adsorbed molecules on electrode surface. The similarity between the Raman spectra obtained from aqueous solutions[1,2] of TsPc and those obtained when they are adsorbed on the silver electrode and also the similarity between the reflectance spectra[4] from the adsorbed Co– and Fe–TsPc on various electrode interfaces and the UV–visible absorption spectra from the same molecules in solution phases are convincing reasons to assume that the symmetry of the macrocycle molecules does not change during the process of the adsorption.

The behavior of the spectra in Figure 7 are explained by a model which involves preferentially orientated adsorbed molecules. According to Sharp and Lardon,[40] the dipole moment of a phthalocyanine molecule lies in its plane. When the electric field component of the incident laser radiation and the induced dipole are parallel, then the corresponding Raman component should be of the strongest intensity. This effect happens only in the case where the electrode surface normal is in the plane of the electric field of incident laser radiation, and consequently the molecular induced moment must be parallel or slightly tilted to the electrode normal. This indicates that the molecule assumes the edge-on rather than a face-on or parallel orientation relative to the electrode surface in the case of the first adsorbed TsPc layer (or in the case of an adsorbed monolayer). On the other hand, one may assume that the surface microroughness on the atomic scale and molecular anisotropy are the causes of the buildup of the Raman I_{SS} and I_{SP} components, and, therefore, the molecular orientation relative to the electrode surface cannot be determined with a certainty. If the anisotropy of the TsPc and its parallel orientation play a major role in providing I_{SS} and I_{SP} components, then such components should be of considerable intensity even on an ideally flat silver substrate at the atomic level.

For such an ideally planar electrode surface and an edge-on molecular orientation, the I_{SS} and I_{SP} components would be zero. Recent experimental data from this laboratory[41] obtained from adsorbed Fe–TsPc on low-index single-crystal silver surfaces show almost nonexistent I_{SS} and I_{SP} components. This experimental evidence excludes contributions from the molecular anisotropy and a possible molecular parallel orientation on the surface. Therefore, the surface roughness on the microscale is a major factor in the production of I_{SS} and I_{SP} Raman scattering components for the adsorbed TsPc even when these molecules are edge-on orientated.

The set of the experimental data in Figure 7 can be explained by the proposed bent model displayed in Figure 8.

The model assumes that the first layer on the silver surface is orientated normally to the surface in the presence of the double-layer potential and that subsequent layers bend and provide parallel molecular orientation.

(38) Krishnan, R. S. *Proc. Indian Acad. Sci.* **1934**, A1782, **1938**, *A7*, 21.
(39) Goncher, G. M.; Persons, C. A.; Harris, C. B. *J. Phys. Chem.* **1984**, *88*, 4200–4209.
(40) Sharp, J. H.; Lardon, M. *J. Phys. Chem.* **1968**, *72* (9), 3230–3235.
(41) Adzic, R. D.; Simic-Glavaski, B.; Yeager, E., unpublished results. And: *Electrochem. Soc. Ext. Abst.* **1984**, *84-1*, 597–598.

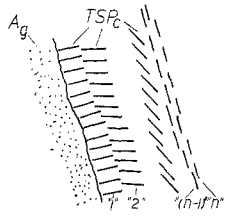

Figure 8. Schematic presentation of the multilayered bent model of the adsorbed tetrasulfonated phthalocyanines on the Ag electrolyte interface. *n* indicates the number of the layer.

Table II. Ratios of $I_{o.p.4}/I_{i.p.28}$

		pH 1	pH 7	pH 13
10^{-5} M Fe–TsPc + electrolyte	S	0.82	0.77	1
	P	0.78	0.78	0.90
$\sim 10^{-10}$ M/cm^2 Fe–TsPc/Ag	S	0.65	0.76	0.84
	P	0.55	0.73	0.72
10^{-5} M Co–TsPc + electrolyte	S	0.34	0.34	1.22
	P	0.20	0.25	0.28
$\sim 10^{-10}$ M/cm^2 Co–TsPc/Ag	S	0.32	0.20	0.26
	P	0.18	0.18	0.22

The intensities of the Raman components in Figure 7a are expected for such a multilayered structure, and the spectra in Figure 7 are highly sensitive to laser polarization. For the spectra in Figure 7b, one may assume that for Ag|(Fe–TsPc)$_{100-n}$|electrolyte, the multilayered structure slowly disappears and changes with time by losing the layers which are in contact with electrolyte. Finally, when all layers are dissolved except the one next to the electrode surface, one obtains Raman components like these in Figure 7c which are also identical with the spectra obtained from an electrochemically adsorbed monolayer where I_{PS} and I_{PP} are the strongest components and approximately equal.

A qualitative analysis of the out-of-plane and the in-plane vibrational modes of the phthalocyanine molecules in aqueous solution phases shows a random orientation while an analysis of these molecules adsorbed on the electrode surface also indicates a molecular preferential orientation.

The ratio of the Raman band intensities for the out-of and in-plane vibrational modes I_{op}/I_{ip} appears to be more descriptive than the relative changes in the intensity of their individual modes. Bands 4 and 6 and 22 and 28 (see Table I) were used in such an analysis. These modes were selected because they are most representative for the out-of-plane and in-plane vibrations, respectively.

The ratios I_{op}/I_{ip} were calculated from the experimental data, and they are summarized in Table II. The appropriate incident laser polarizations S and P together with pH values of the supporting electrolyte are indicated in the Table II.

The other vibrational modes yield similar results. The reduced ratios for the P-polarized laser light in the examples for the adsorbed Co–TsPc and Fe–TsPc on the silver electrode indicate an enhancement of the in-plane vibrational modes or a reduction in the intensity of the out-of-plane vibrational modes. The values of the intensity ratios also support a model in which the TsPc molecules have an edge-on orientation relative to the electrode surface.

Previously offered hypotheses of phthalocyanine molecules being parallel to the electrode surface, proposed by Melandres et al.,[15] cannot be supported by our data.

Relatively small ratio differences for the S and P polarization data can be explained as a consequence of behavior of the axially symmetric attachment of water molecules to a phthalocyanine species. Under such circumstances, the direction of the out-of-plane vibrations can be altered substantially in a direction which is more colinear with the molecular plane.

Prior experimental data obtained by the surface tension technique[42] also favor the edge-on orientation for iron and magnesium

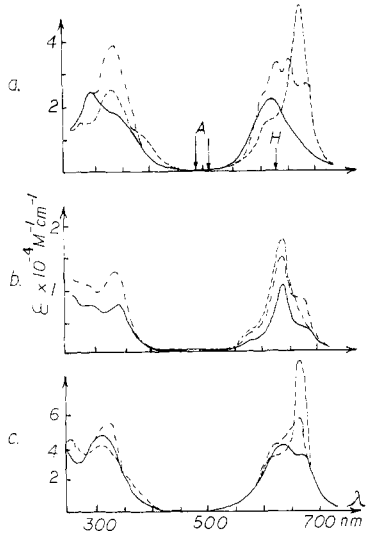

Figure 9. UV–visible absorption spectra obtained from aqueous 10^{-5} M solution phases of (a) H_2–TsPc, (b) Fe–TsPc, and (c) Co–TsPc in 0.05 M H_2SO_4 (—), 0.05 M Na_2SO_4 (-·-·-), and 0.1 M NaOH He (---) saturated electrolytes. The argon ion A and the He–Ne H laser excitation lines are indicated by arrows. T = 20 °C.

phthalocyanine monolayers on water interfaces and indicate a covered area of 50 Å^2/molecule rather than the 130 Å^2/molecule necessary for a parallel orientation. Other measurements and the experimental evidence[43] show similar orientation for chlorophyll molecules adsorbed on SnO_2. It may be also possible that the first layer of the adsorbed TsPc on a solid substrate is arranged as close-packed tilted *J* aggregates which have been previously reported for 2,2′-cyanine dyes molecules.[44] On the other hand, the experimental data of Buchholz and Somorjai[45] are interpreted as indicating that molecular orientation is parallel for the epitaxially grown monolayer of vapor-deposited phthalocyanines on copper. Some other experimental conditions may significantly influence the orientation of the adsorbed molecules. The relatively intense I_{SS} component for the adsorbed H_2–TsPc on the silver electrode in neutral electrolytes may also indicate a parallel molecular orientation. The change of the H_2–TsPc orientation in neutral media can be closely related to the distinctly lowered molecular D_{2h} symmetry.

3. Influence of the Laser Excitation Frequency. The study of the UV–visible spectra from TsPc in aqueous media was performed parallel to this work. A detailed analysis of absorption spectral properties of aqueous solutions of TsPc interpreted in terms of molecular orbital theory will be reported elsewhere.[46] The principal UV visible absorption spectra recorded from the aqueous solutions of 10^{-5} M TsPc are displayed in Figure 9. The UV Soret B and visible absorption Q bands originate from the π–π^* electronic transition. Metallophthalocyanines as well as their corresponding sulfonated molecular species belong to the D_{4h} symmetry group, while metal-free TsPc in neutral media has a lowered D_{2h} symmetry with characteristic splitting of the visible Q bands. Deprotonated and additionally protonated H_2–TsPc in alkaline and acidic media assume higher D_{4h} symmetry. In general, Raman spectra are dependent on the wavelength of the laser excitation when the laser line approaches dispersive absorption ranges. Prior detailed studies on similar molecules such as porphyrins show a close resemblance between the Raman line intensity excitation profile and the absorption spectra. According to Spiro,[25] a laser excitation line which is near the Soret band enhances totally symmetric modes of the macrocycle molecules which are in the range between 1100 and 1650 cm^{-1}, while the laser excitation near

(42) Alexander, A. E. *J. Chem. Soc.* **1937**, 1813–1819.

(43) Miyasaka, T.; Watanabe, T.; Fujishima, A.; Honda, K. *Nature (London)* **1979**, *277*, 638–640.
(44) Scheibe, G. *Z. Elektrochem.* **1948**, *52*, 283–292.
(45) Bucholz, J. C.; Somorjai, G. A. *J. Chem. Phys.* **1977**, *66* (2), 573–580.
(46) Simic-Glavaski, B.; Zecevic, S.; Yeager, E., unpublished results. And: *Electrochem. Soc. Ext. Abst.* **1984**, *84-1*, 566–567.

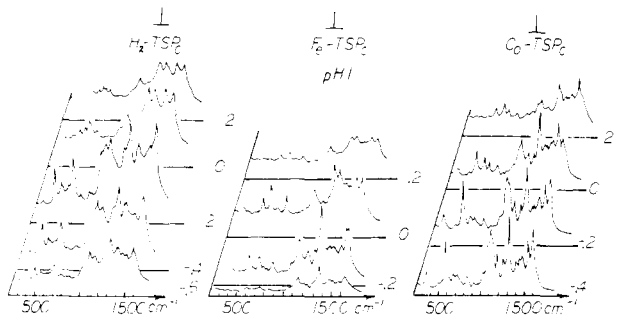

Figure 10. Surface-enhanced Raman spectra from the adsorbed H_2–, Fe–, and Co–TsPc on the silver electrode when the adsorbed molecular species were illuminated with the argon ion line at 514.5 nm with an output power of about 100 mW. The polarization of the scattered light is shown in Figure 1b. The spectra were obtained from the adsorbed macrocycle molecules in the He saturated acidic medium. Resolution 2 cm^{-1}; scan rate 10 min/spectrum.

the Q absorption bands enhances nontotally symmetric modes in the lower frequency range.

Laser excitation lines at 488 and 514.5 nm were also used for recording the SER spectra from the adsorbed TsPc as a function of the electrode potential. The depolarized spectra obtained with 514.5-nm laser line from the studied macrocycle molecules are displayed in Figure 10.

The shapes of the Raman spectra are considerably altered with a relative enhancement of the higher frequency range which is in good agreement with the previously reported findings for porphyrins.[25] The number of Raman lines was independent of the laser excitation, and intensity ratios for I_{ps}/I_{ss} of ~ 2 are similar to these values already shown in Figures 3, 4, and 5.

The available laser excitation lines shown in Figure 9 which were used to excite the adsorbed TsPc have positions which make difficult a detailed analysis of the vibrational band intensities vs. the wavelength of the laser excitation. The wavelengths of these laser lines do not warrant any sensible analysis of the excitation profiles as a function of the laser excitation wavelength. Furthermore, the experimental data obtained in this work, with practically only two laser excitation lines, are not sufficient to critically evaluate the controversial issue[47-50] of Raman scattering from macrocycle molecules as a function of the laser excitation frequency.

4. Dependence of Raman Scattering on the Electrode Potential. (a) Frequency Shift of Raman Bands. Numerous reports on SERS[6-11] show changes as a function of the electrode potential in both the intensity and in the position of Raman bands. The frequency shifts of the Raman bands from the adsorbed TsPc as a function of electrode potential were examined individually with higher resolution. Most of the frequency changes were less than the error of the measurements (2 cm^{-1}). Only the bands at about 763, 612, and 506 cm^{-1} showed appreciable frequency changes for Co–, Fe–, and H_2–TsPc, respectively, in acidic electrolytes as shown in Figure 11.

The position of the Raman band at 1347 cm^{-1} from Co–TsPc in alkaline media changes very little as a function of the electrode potential.

It was also determined experimentally that frequency shifts of the particular Raman bands are functions of the laser excitation (see Figure 11) and pH as displayed in Figure 12.

The frequency shift of the Raman lines as a function of the electrode potential appears to be a measure of the ionization of the phthalocyanine molecules. Aleksandrov et al.[13] observed a frequency shift of some Raman lines which they attribute to the ionization of the MPc. According to their study, the frequency shift of the Raman lines toward the lower wavelengths is proportional to the degree of ionization of the metal ion. It is significant that the changes in the frequency shift are most pronounced in the ranges of the redox potentials of the macrocycle molecule.

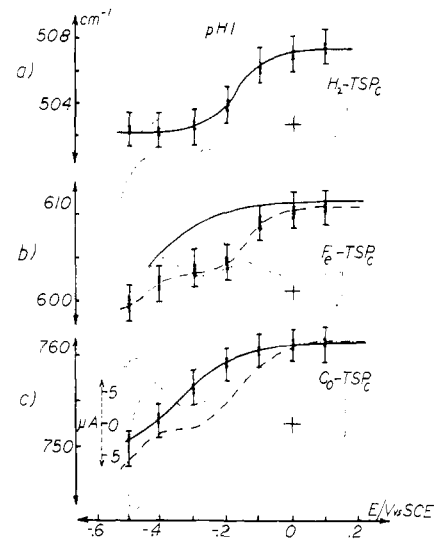

Figure 11. Frequency shifts in inverse centimeters of the Raman bands as a function of the electrode potential for the adsorbed (a) H_2–, (b) Fe–, and (c) Co–TsPc on the silver electrode in acid (pH ~ 1) electrolyte. The full and dashed dotted lines were obtained with 632.8- and 514.5-nm laser illumination, respectively. Dotted curves represent appropriate cyclic voltammograms obtained with a potential scanning rate of 100 mV/s for easier peak identification. The abscissa of the electrode potential is in volts vs. SCE. The error bar represents the resolution of the monochromator.

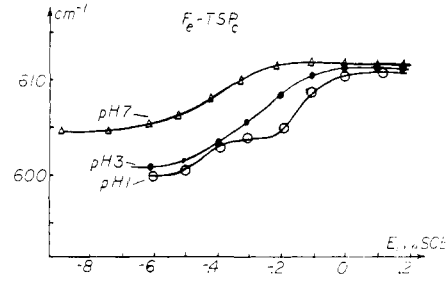

Figure 12. Variation of the frequency shift of the 612-cm^{-1} Raman band for Fe–TsPc as a function of the electrode potential at different pH values. The laser excitation was 514.5 nm.

The frequency shift of the Raman band at about 612 cm^{-1} for Fe–TsPc at pH ~ 1 obtained with the argon line at 514.5 nm is of particular interest since it can be directly correlated with the redox peaks (see Figure 11b). The two inflection regions observed correspond very well with the redox potentials and appear to be sensitive and specific indicators of oxidation processes involving Fe–TsPc at pH ~ 1. The Raman band at about 612 cm^{-1} for Fe–TsPc probably represents the pyrrole out-of-plane folding mode and is therefore related to the iron vibration in Fe–TsPc molecules. This folding mode appears to strongly affect the C–N bond at 1346 cm^{-1} which shows most interesting behavior when the intensity of the Raman band is measured as a function of the oxidation–reduction cycle. These phenomena will be discussed in greater detail below. The frequency shifts of the Raman bands were measured against the applied electrode potential when pH was taken as a constant parameter. The measured differences in the frequency shift of the Raman bands as a function of pH are consistent with the potential variation of the oxidation–reduction peaks as a function of pH.[18] However, these variations in frequency shift changes are smaller for higher pH values. It should be noted here that the inflection regions in Figure 11b are within the resolution of the monochromator. Only repeated measurements could provide the clustered values of the Raman band positions which were less dispersed than the error margin.

(47) Warshel, A.; Dauber, P. *J. Chem. Phys.* **1977**, *66*, 5477–5488.
(48) Albrecht, A. C. *J. Chem. Phys.* **1961**, *34*, 1476–1484.
(49) Peticolas, W. L.; Nafie, L.; Stein, P.; Fanconi, S. *J. Chem. Phys.* **1970**, *52*, 1576–1584.
(50) Behringer, J. *J. Mol. Spectrosc.* **1974**, *28* 100–172.

The variations in frequency shifts as a function of the electrode potential and the laser excitation can be explained on a rather general basis. It has already been demonstrated for porphyrin molecules that the polarizability tensor[25] exhibits two maxima as a function of the wavelength of the incident laser radiation. It may also be assumed that the same factor is valid for phthalocyanines. In addition, the electronic absorption spectrum obtained from phthalocyanines is a function of the electrode potential. For adsorbed lutetium diphthalocyanine on tin oxide electrodes, Moskalev et al.[51] noticed that the position of the absorption maxima shifted as a function of the electrode potential, and the absorption Q band maxima changed its position toward the wavelength as the cathodic potential was increased.

In the recently published works of Lever et al.[52] and Harriman et al.,[53] the experimental data show a photoreduction process of

$$Mn^{III} \xrightarrow{h\nu} Mn^{II}\text{–TsPc}$$

and the formation of π-radical cations in illuminated aqueous solutions of metalloporphyrins, respectively.

One of the possible photoreduction schemes involves a probable acid–base transition of the axially coordinated water molecules and the formation of an hydroxide ion according to the scheme

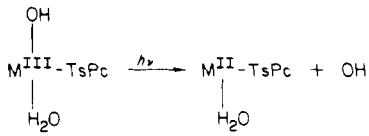

A high frequency cutoff is ~520 nm for the above mechanism. However, this hypothetical mechanism, though probable, must still be considered highly speculative in the absence of the other supporting evidence. This may explain the rather unusual effect that the frequency shifts of the Raman bands are a function of the electrode potential and are also a function of the incident laser radiation.

Nonresonant or out-of-Q or -B laser excitation is more convenient for following the electrochemical parameters of the adsorbed macrocycle species than is the resonant laser excitation methodology. When the laser excitation approaches vibronically active modes and allowed electronic transitions and at the same time the electrochemical processes perturb the system, then it is experimentally very difficult to separate electrochemical from photoeffects.

(b) Raman Oxidation–Reduction Cycle. The Raman spectra obtained from the TsPc adsorbed on the silver electrode shown in Figures 3, 4, and 5 are substantially dependent on the electrode potential. The intensity change of the Raman bands vs. electrode potential can be studied in a continuous potential sweeping mode rather than in discrete potential steps.

This methodology for obtaining a direct correlation between electrochemical redox processes and the surface-enhanced Raman signals for the adsorbed TsPc on the silver electrode was reported earlier.[5] In this way, one measures in parallel the electrochemical oxidation–reduction cyclic voltammograms and the changes of the optical signal which we call Raman ORC (oxidation–reduction cycle). The shapes of the Raman ORC's are invariant to the adsorption procedure of TsPc molecules on the electrode surface. The corresponding Raman ORCs are of the same shape and intensity regardless of whether the macrocycle molecules had been adsorbed during or following the electrode activation. This fact also indicates that the origin and properties of the Raman ORC's are only a function of the adsorbed macrocycle behavior in a continuously variable electric field of the electrode interface.[5] Most importantly, Raman ORC's can provide specific answers as to which parts of the molecule are associated with, or responsible for, oxidation–reduction peaks.

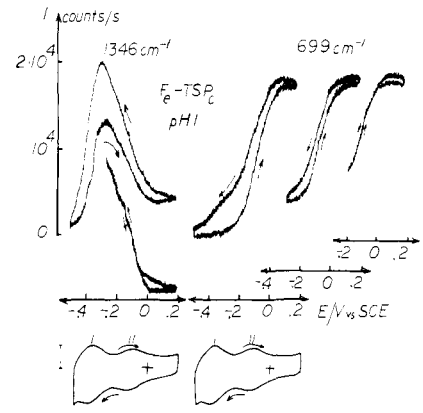

Figure 13. Raman ORC's for 1346- and 699-cm^{-1} Raman bands obtained from Fe–TsPc adsorbed on the silver electrode in 0.05 M H_2SO_4 electrolyte. The scan rate of the Raman ORC's was 10 mV/s, and the laser excitation was 514.5 nm. The vertical bar represents a change in the signal intensity of the Raman band in counts/second. Cyclic voltammograms from Fe–TsPc adsorbed on the silver electrode were obtained with the potential scan rate of 100 mV/S. The dotted vertical bar is 10 μA. The Raman ORC's were obtained with the depolarized Raman scattered light.

Only the relevant data not previously described will be discussed in this paper. In the example for Fe–TsPc adsorbed on the silver electrode in an acidic electrolyte, 0.05 M H_2SO_4 (pH ~1) (see Figure 13) yields Raman ORC's which are accompanied by a pronounced hysteresis when the potential sweep is performed between the limits of hydrogen evolution and silver dissolution. The hysteresis can be eliminated if the electrode potential sweeping window is limited from +0.2 V to the potential value of the first redox peak (see Figure 13). The Raman ORC's were measured in both the polarized and depolarized light scattering modes and no significant differences were observed in their shape. However, the hysteresis areas were not identical; this may have been due to a different orientation of the characteristic vibrational mode and its relative orientation to the plane of the incident laser polarization and thus to the molecular orientation on the electrode surface. It should be pointed out that the recorded Raman spectra in discrete potential steps and the Raman ORC's obtained in a continuous potential sweeping mode were completely reversible if the potential of the electrode performed a full oxidation–reduction. It was verified experimentally that the Raman ORC's and their hysteresis are not a result of the adsorption–desorption mechanism and the fluorescence background effects which also showed some degree of intensity modulation as a function of the electrode potential. The Raman ORC's can be also reconstructed from the intensity levels of the Raman bands recorded at constant potentials providing that the potential stepping was in the same direction as the direction of the cyclic voltammograms.

The shape of the Raman ORC's is dependent on the laser excitation frequency. These differences can be accounted for by the response of the polarizability tensor as a function of the excitation wavelength and may be quite distinct in the nonresonant and resonant dispersive regimes. In the latter case, when the laser excitation falls in a dispersive region of the molecular polarizability, the influence of the electrode field is less pronounced than the inherent molecular properties, and hence resonant effects appear to be stronger for M–TsPc than the competitive electrochemical processes. The electrochemical processes appear far more predominant for the nonresonant laser excitation of the adsorbed species. The changes in the Raman ORC's follow much better the redox mechanisms observed in the cyclic voltammograms, as was already discussed with respect to the effect of the frequency shifts as a function of the laser radiation. However, one should be aware that the highly complex structure of the macrocycle molecules can support photoeffects, photoinduced catalysis[54]

(51) Moskalev, P. N.; Kirin, I. S. *Opt. Spectrosc.* **1970**, *29*, 220–221.
(52) Lever, A. B. P.; Licoccia, S.; Ramaswamy, I. *Inorg. Chim. Acta* **1982**, *64*, L87–L90.
(53) Harriman, A.; Porter, G.; Walters, P. *J. Chem. Soc. Faraday Trans.* **1983**, *798* 1335–1350.
(54) Gurevich, M. G.; Solovev, K. N. *Dokl. Akad. Nauk BSSR* **1961**, *58* 291–198.

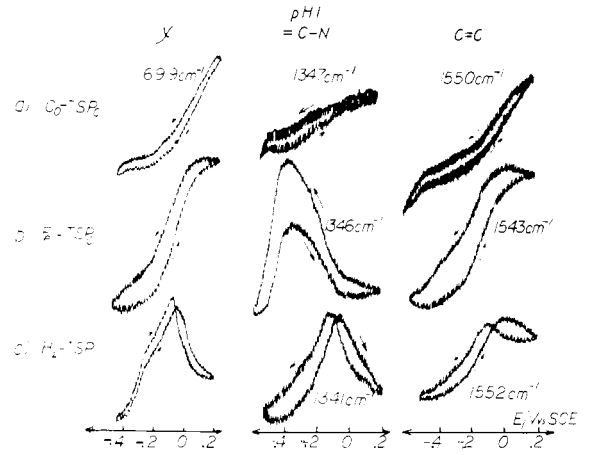

Figure 14. Relative comparison of the Raman ORC's obtained from adsorbed (a) cobalt, (b) iron, and (c) metal-free TsPc on the silver electrode in 0.05 M H_2SO_4 electrolyte. The Raman bands at 699, 1347, and 1550 cm^{-1} represent characteristic common vibration for all three phthalocyanines. The curves were obtained with the potential scan rate of 10 mV/s. The optical polarization of the Raman ORC's is the same as in Figure 13.

pronounced fluorescence,[55] and luminescence[56] and that all these phenomena may be simultaneously involved in some instances.

The Raman ORC's obtained from the adsorbed TsPc can be classified mainly in two groups according to their shape. In the first group (see Figure 13), Raman ORC's of the bands at 387, 612, 699, 866, 1392, and 1543 cm^{-1} show a gradual change with the applied potential and do not correlate so directly with the redox peaks in cyclic voltammograms. In the second class, there is a pronounced maximum associated with the Raman bands at 1346 and 1136 cm^{-1}. The maxima of the Raman ORC's appear at the same potentials as cyclic voltammogram peak I, and thus it is possible to analyze the origin of the redox peak I more closely and correlate it with the given tentative band assignment. The common changes in the ν_r, ν_X, and C=C vibrational modes at the oxidation potentials of peaks I and II suggest an oxidation of the pyrrole ring and a delocalized charge within the ring. Raman ORC's were also measured for H_2- and Co-TsPc, with the results suggesting the involvement of a similar process.

This type of analysis utilizing the Raman ORC's provides deeper insight into potential assignment of possible sites where oxidation or reduction can take place even in such complex molecules. Cyclic voltammetry alone fails to provide such specificity.

The interaction of the central metal atom with the phthalocyanine ring can be analyzed through observation of the Raman ORC of characteristic Raman bands. Although specific metal vibrational bands could not be assigned with certainty, indirect observation of the distortion of the pyrrole ring and the corresponding atomic bonds could be used as the basis for an analysis of the behavior of the central metal atom. The Raman ORC's of the bands at about 699, 1346, and 1550 cm^{-1}, representing pyrrole ring deformation and N—C and C=C vibrational modes, respectively, are shown in Figure 14 for Co-, Fe-, and H_2-TsPc and are used in such an analysis. The difference in the Raman ORC's can be explained in terms of specifc metal or proton vibrations. The Co ion vibrates largely in the plane of the TsPc inner ring while the Fe ion can assume a high spin domed or low spin planar configuration, thus grossly affecting the vibrational bands of the pyrrole ring and, as a consequence, the Raman ORC's. The Raman ORC's for Co- and Fe-TsPc show changes which correspond to both the cycling voltammogram peaks I and II. A change of the electrolyte pH value can produce drastic changes in the Raman ORC's as shown in Figure 15 for the case of adsorbed Fe-TsPc. Two Raman bands have been chosen to illustrate pH effects together with the electrode potential and are

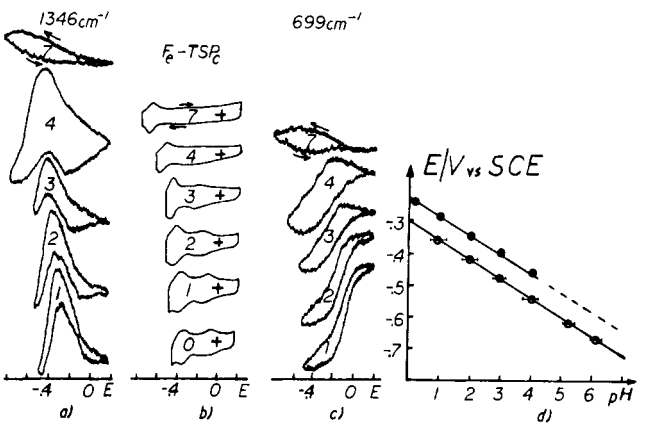

Figure 15. Raman ORC's for the bands at (a) 1346 cm^{-1} and (c) 699 cm^{-1} obtained from the adsorbed Fe-TsPc on the silver electrode for various values of pH. The Raman ORC's were obtained with the potential scan rate of 10 mV/s and 514.5-nm laser excitation with normal polarization. The curves b show the cyclic voltammograms obtained from the adsorbed Fe-TsPc on the same silver electrode; pH values of the electrolytes are indicated. In order to obtain pronounced voltammogram peaks, a scan rate of 100 mV/s was used only for convenience. Figure 15d shows a potential variation of the cyclic voltammogram peaks I (○), and the position of the maxima obtained from Raman ORC (●), for the band at 1346 cm^{-1} for various values of pH. The slopes of the lines are 60 mV/pH unit.

correlated with the simultaneously measured cyclic voltammograms. The experimental data for the adsorbed Fe-TsPc show that the hysteresis is directly proportional to the pH values (Figure 15). Other Raman bands from Co- and H_2-TsPc adsorbed on the silver electrode yield similar effects.[5] The experimental results indicate a direct proportionality between the hysteresis and the bulk or surface pH value of the electrolyte.

The potential position of the maxima in the Raman ORC's is associated with a characteristic shift of about 60 mV per pH unit; the values are identical with the values obtained from cyclic voltammetry. However, the potential positions of the Raman ORC's maxima are shifted about 70 mV toward the anodic potential and coincide with the half height of the corresponding cyclic voltammogram peak.

It appears that the electrode potential and pH simultaneously produce a charge transfer in the adsorbed TsPc. The dependence of the wavelength position of the absorption maximum as a function of the electrode potential, as discussed earlier, suggests that d-orbital electrons are closely associated with the phenomenon of a delocalized electron in the pyrrole ring.

Conclusions

The analysis of the recorded in situ Raman data from the TsPc adsorbed on the silver electrode reveals several important and significant features as well as number of new phenomena.

Metal-free tetrasulfonated phthalocyanine in aqueous solution showed a strong fluorescence background; however, when H_2-TsPc was adsorbed on the silver electrode, the fluorescence was quenched and strong Raman spectra could be obtained. These spectra were used in a comparative analysis of the Raman data obtained from other adsorbed and solvated TsPc. This approach provided a means of producing tentative band assignments. The strongest Raman bands are associated with the pyrrole vibrations and the C—N and C=C vibrational modes.

However, a specific metal vibrational mode could not be identified with certainty, although the specific ion behavior in the inner ring strongly influences the prominent associated Raman bands. Such effects allow detailed analysis of the adsorbed macrocycle species on interfaces. In addition, the Raman spectra obtained from TsPc are similar to those obtained from porphyrins, hemoglobin, and cytochrome *c*.

The great similarity between the Raman spectra obtained from adsorbed TsPc on the silver electrode and those spectra obtained from solution phases of TsPc and from crystalline Pc show that (i) the adsorbed molecular species do not change molecular

(55) Seybold, P. G.; Gouterman, M. *J. Mol. Spectrosc.* **1969**, *31*, 1–13.
(56) Vincent, P. C.; Voight, E. M.; Rieckoff, K. E. *J. Chem. Phys.* **1971**, *55*, 4131–4140.

symmetry during the process of the adsorption, (ii) the influence of sulfonic groups is minimal or negligible on the overall behavior of Pc molecules, and (iii) the TsPc molecules adsorbed on the silver electrode are adsorbed mainly through the phys- rather than chem-adsorption mechanism. In addition, use of the incident laser polarization information and the recorded polarized and depolarized Raman spectra from adsorbed TsPc on a silver electrode suggests an edge-on molecular orientation.

The laser excitation in the adsorption Q bands provides resonant SERS but at the same time indicates photoeffects. Nonresonant laser excitation of the adsorbed TsPc appears more suitable for studying electrochemical processes and provides very specific answers in the case of adsorbed monolayers on the electrode interfaces.

Raman ORC's obtained by using SERS simultaneously with cyclic voltammetry allow detailed analysis of the oxidation-reduction process in TsPc. Such studies have a significant bearing on the analysis of the oxidation of TsPc and most probably of the behavior of heme molecules in the presence of oxygen molecules. The Raman ORC's reported here indicate that pyrrole ring electrons are delocalized and that Raman ORC's can provide assignment of the cyclic voltammogram peaks.

The experimental data presented also show a direct correlation between the Raman scattering effect and an electrochemical process; this may prove to be a very powerful analytical methodology.

Acknowledgment. We thank DOE for partial support of this work, and B. S.-G. thanks Dr, D. Schuele and S. S. for financial help.

Registry No. H_2-TSPc, 19497-02-0; Co-TSPc, 29012-54-2; Fe-TSPc, 86508-34-1; Ag, 7440-22-4.

Role of Excited Atomic States in the Active Sites of Transition Metals for Oxidative and Reductive Catalytic Processes

J. García-Prieto,[†] M. E. Ruíz,[†] and O. Novaro*[‡]

Contribution from the Instituto Mexicano del Petróleo, Investigación Básica de Procesos, A.P. 14-805 México 07730 D.F., Mexico, and Instituto de Física, U.N.A.M., A.P. 20-364 México 01000 D.F., Mexico. *Received November 20, 1984*

Abstract: Model potential configuration-interaction calculations using a variational reference state of ~100 configurations and a Møller-Plesset perturbational study including another ~750 000 configurations are addressed in the study of a model for the oxidative and reductive processes that occur at a metallic copper catalyst. The main goal is to show the central role that is played by the excited states of a transition metal, since without their detailed knowledge, one may grossly overestimate the activation barrier for the H-H bond breaking in the chemisorption process of a H_2 molecule. The potential energy surfaces relevant to the study of the oxidative and reductive processes include those used before in the study of the photochemical reaction of a Cu atom with a H_2 molecule at matrix isolation conditions and also additional calculations for a total three-dimensional image of these important potential energy surfaces. We also study the relative minima for the intermediate CuH_2 system, which is unobservable for the photochemical process as reported elsewhere, but very crucial here as a model of the chemisorbed species of the oxidative and reductive catalytic processes. In consequence a very detailed description of the bent and linear geometries of the CuH_2 complex is given, with emphasis on the molecular orbital structures, charge transfer, etc. From all this we conclude that two possible chemisorbed forms of H_2 on copper exist: one with a very weak H-H bond, another with only atomic hydrogen on the copper sites. Our calculations predict an energy barrier for chemisorption of 28 kcal/mol, virtually identical with the experimental dissociative adsorption energy for H_2 on copper.

I. Introduction

It has now been quite some time since the first proposal[1] to correlate data on "naked" metal atoms or "naked" metal clusters with those of the actual surface of a heterogeneous catalyst was advanced. This was based on a wealth of experimental data available from a matrix isolation technique[2] and led to the very tempting idea of tailor-making reaction intermediates that ought to reproduce (or model) the actual chemical situations through a catalytic cycle. It should be mentioned that this is a different concept from the "catalyst tailoring" approach in homogeneous catalysis.[3]

About the same time, the first proposals for using ab initio studies of metal cluster complexes[4] to understand the chemistry of metal surfaces were advanced, and also many semiempirical molecular orbital studies were carried out.[5] The latter are, of course, greatly limited by their use of empirical data to really give significant and independent predictions to the catalytic phenomena. As concerns the ab initio approach, they have concentrated mostly on building large enough (nontransition) metal clusters[6] to represent reasonably well the collective electronic properties of infinite surfaces, in spite of continuous warnings, such as those of Moskovits[7] that collective phenomena do not correlate per se with molecular adsorption in the limit of small particles. We have proposed elsewhere a different way to go into the question of how collective effects can be evaluated for finite clusters.[8]

[†] Instituto Mexicano del Petróleo.
[‡] Instituto de Física.

(1) Ozin, G. A. *Acc. Chem. Res.* **1977**, *10*, 21.
(2) (a) Ozin, G. A. *Catal. Rev.-Sci. Eng.* **1977**, *16*, 191, and references cited therein. (b) Ozin, G. A. *Coord. Chem. Rev.* **1979**, *28*, 117, and references cited therein.
(3) Olivé, S.; Henrici-Olivé, G. "Homogeneous Catalysis"; Elsevier: Zurich, 1978.
(4) (a) Schaefer, H. F. *Acc. Chem. Res.* **1977**, *10*, 287. (b) Goddard, W. A. *Chem. Eng. News* **1976**, *54*, 14.
(5) (a) Anderson, A. B.; Hoffmann, R. *J. Chem. Phys.* **1974**, *61*, 4545. (b) Schrieffer, J. R. *J. Vac. Sci. Technol.* **1976**, *13*, 335. (c) Mason, M. G.; Baetzold, R. C. *J. Chem. Phys.* **1976**, *64*, 271. (d) Blyholder, G. *Ibid.* **1975**, *62*, 3192. (e) Anderson, A. B. *Ibid.* **1976**, *65*, 1729. (f) Johnson, K. H.; Messmer, R. P. *J. Vac. Sci. Technol.* **1974**, *11*, 236.
(6) (a) Bagus, P. S.; Schaefer, H. F.; Bauschlicher, Ch. W. *J. Chem. Phys.* **1983**, *78*, 1390. (b) Bauschlicher, Ch. W.; Liskow, D. H.; Bender, C. F.; Schaefer, H. F. *Ibid.* **1975**, *62*, 4815. (c) Bauschlicher, Ch. W.; Bender, C. F.; Schaefer, H. F.; Bagus P. S. *Chem. Phys.* **1976**, *15*, 227. (d) Hermann, K.; Bagus, P. S. *Phys. Rev. B* **1978**, *17*, 4082.
(7) Moskovits, M. *Acc. Chem. Res.* **1979**, *12*, 229.

0002-7863/85/1507-5635$01.50/0